YMTHE, Volume *26*

Supplemental Information

microRNA-219 Reduces Viral Load and Pathologic Changes in Theiler's Virus-Induced Demyelinating Disease

Ana Lis Moyano, Jeffrey Steplowski, Haibo Wang, Kyung-No Son, Diana I. Rapolti, Jeffrey Marshall, Vince Elackattu, Michael S. Marshall, Amy K. Hebert, Cory R. Reiter, Viviana Ulloa, Katarzyna C. Pituch, Maria I. Givogri, Q. Richard Lu, Howard L. Lipton, and Ernesto R. Bongarzone

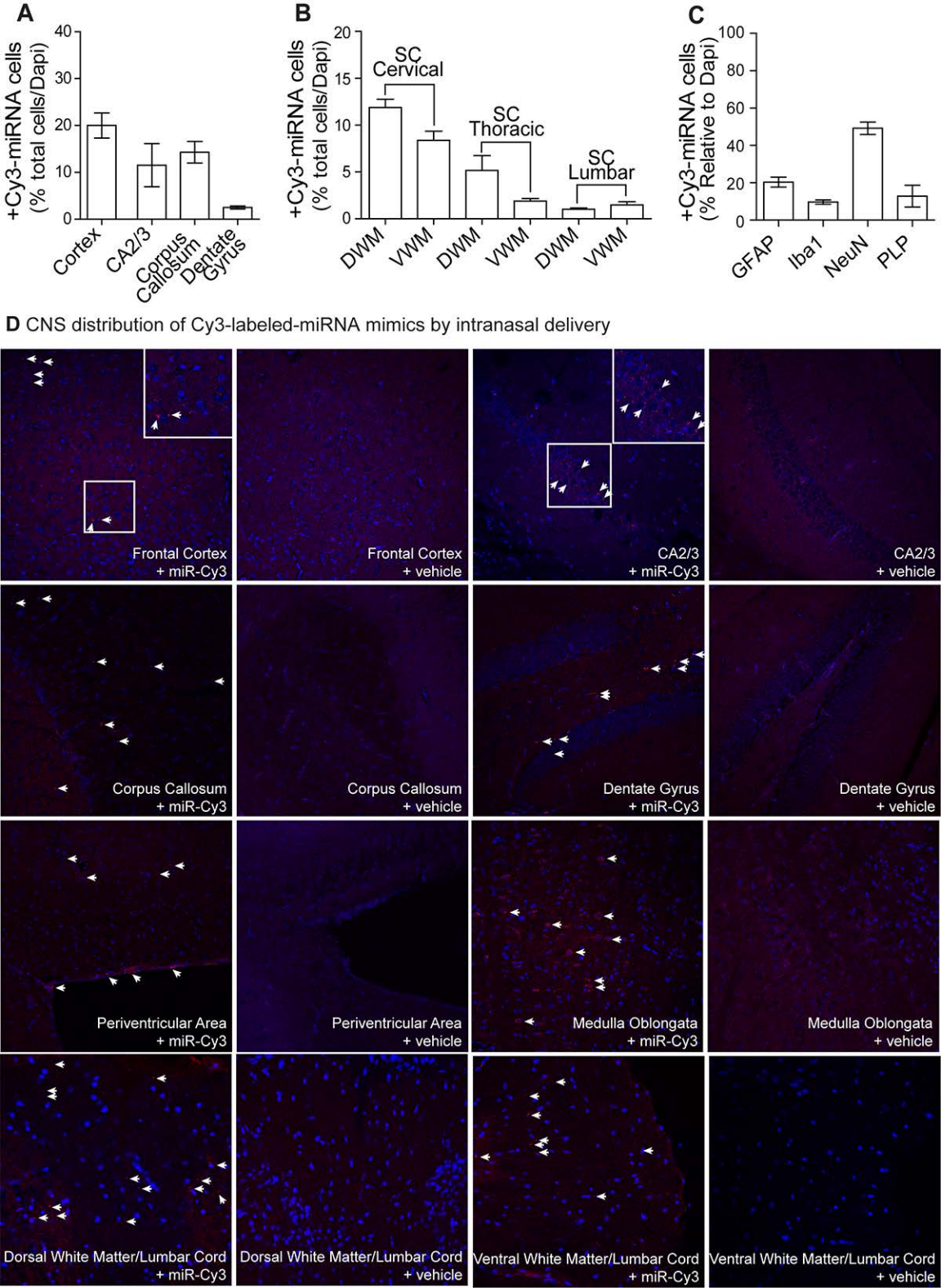
A
+Cy3-miRNA cells
(% total cells/Dapi)
40
30
20
10
0
Cortex
CA2/3
Corpus Callosum
Dentate Gyrus
B
+Cy3-miRNA cells
(% total cells/Dapi)
20
15
10
5
0
SC Cervical
SC Thoracic
SC Lumbar
DWM
VWM
DWM
VWM
DWM
VWM
C
+Cy3-miRNA cells
(% Relative to Dapi)
100
80
60
40
20
0
GFAP
Iba1
NeuN
PLP
D CNS distribution of Cy3-labeled-miRNA mimics by intranasal delivery
Frontal Cortex + miR-Cy3
Frontal Cortex + vehicle
CA2/3 + miR-Cy3
CA2/3 + vehicle
Corpus Callosum + miR-Cy3
Corpus Callosum + vehicle
Dentate Gyrus + miR-Cy3
Dentate Gyrus + vehicle
Periventricular Area + miR-Cy3
Periventricular Area + vehicle
Medulla Oblongata + miR-Cy3
Medulla Oblongata + vehicle
Dorsal White Matter/Lumbar Cord + miR-Cy3
Dorsal White Matter/Lumbar Cord + vehicle
Ventral White Matter/Lumbar Cord + miR-Cy3
Ventral White Matter/Lumbar Cord + vehicle

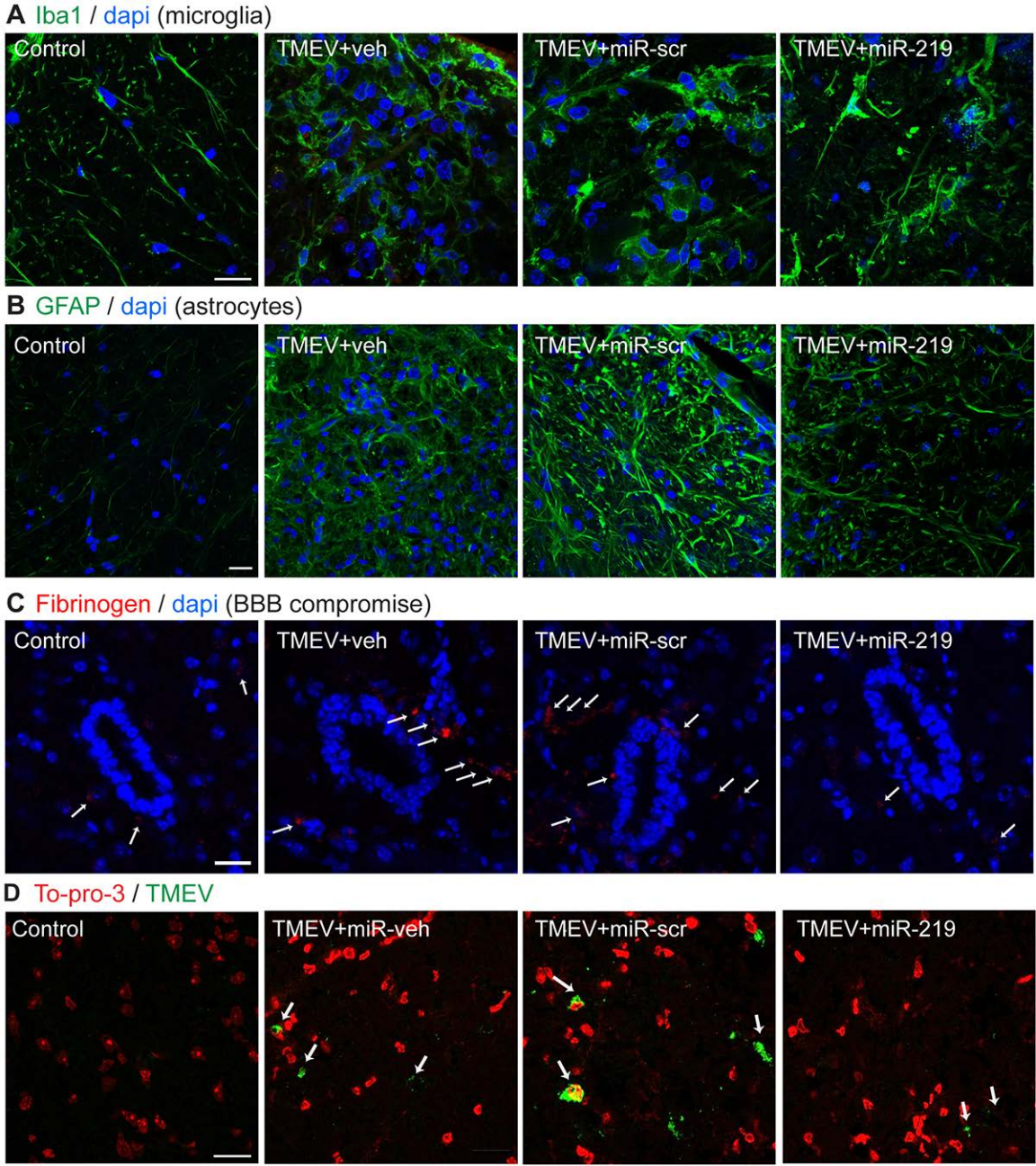
A Iba1 / dapi (microglia)
Control
TMEV+veh
TMEV+miR-scr
TMEV+miR-219
B GFAP / dapi (astrocytes)
Control
TMEV+veh
TMEV+miR-scr
TMEV+miR-219
C Fibrinogen / dapi (BBB compromise)
Control
TMEV+veh
TMEV+miR-scr
TMEV+miR-219
D To-pro-3 / TMEV
Control
TMEV+miR-veh
TMEV+miR-scr
TMEV+miR-219

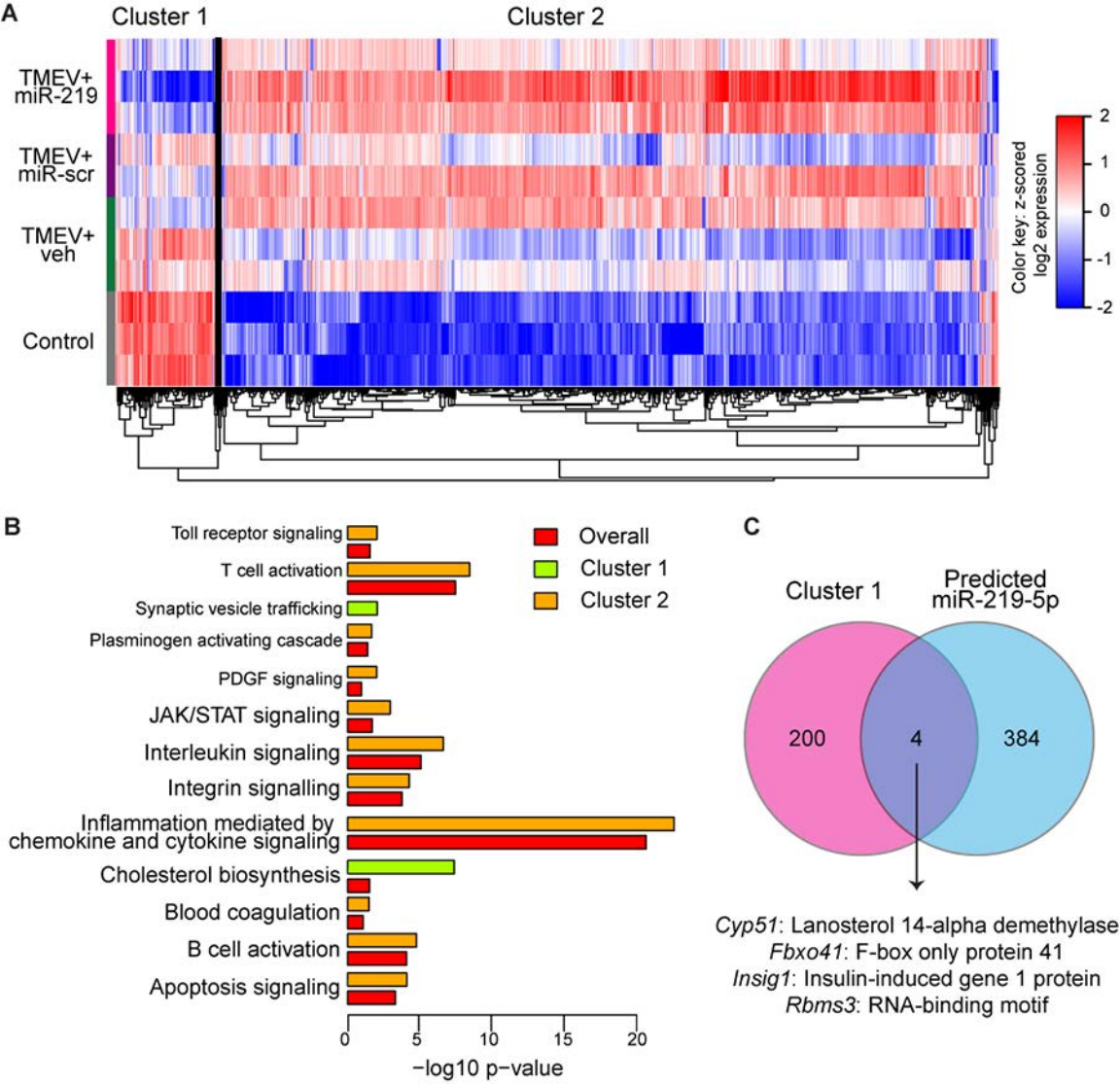
A
Cluster 1
Cluster 2
TMEV+ miR-219
TMEV+ miR-scr
TMEV+ veh
Control
Color key: z-scored log2 expression
2
1
0
-1
-2
B
Toll receptor signaling
T cell activation
Synaptic vesicle trafficking
Plasminogen activating cascade
PDGF signaling
JAK/STAT signaling
Interleukin signaling
Integrin signalling
Inflammation mediated by chemokine and cytokine signaling
Cholesterol biosynthesis
Blood coagulation
B cell activation
Apoptosis signaling
Overall
Cluster 1
Cluster 2
0
5
10
15
20
−log10 p−value
C
Cluster 1
Predicted miR-219-5p
200
4
384
Cyp51: Lanosterol 14-alpha demethylase
Fbxo41: F-box only protein 41
Insig1: Insulin-induced gene 1 protein
Rbms3: RNA-binding motif

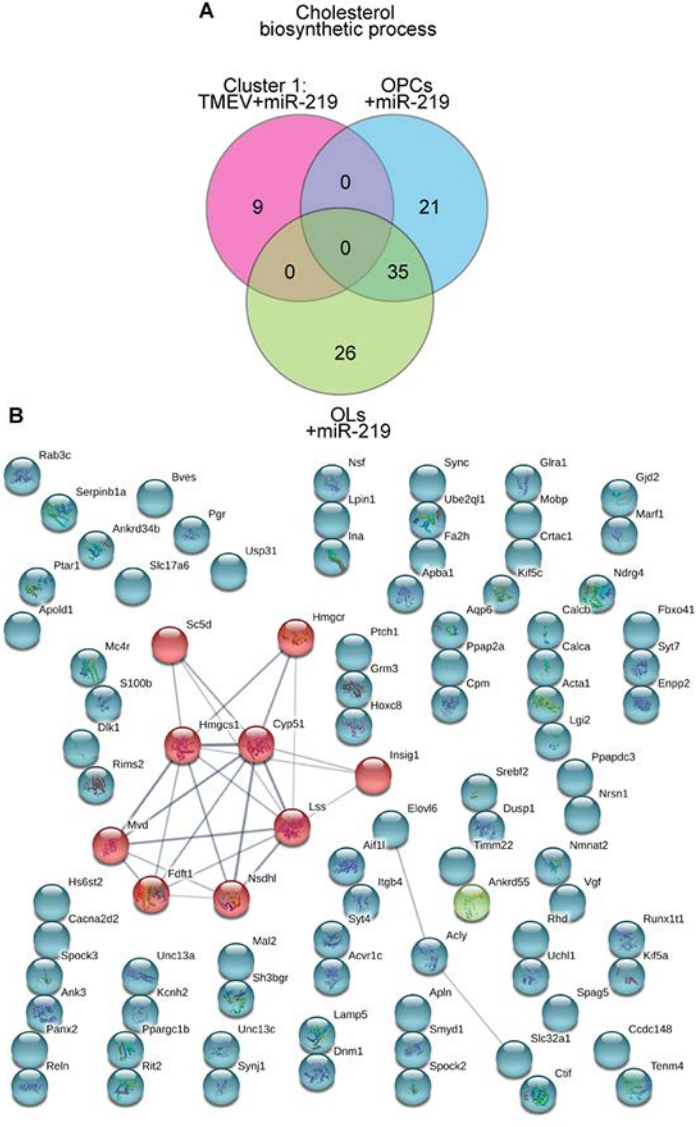
A
Cholesterol biosynthetic process
Cluster 1: TMEV+miR-219
OPCs +miR-219
OLs +miR-219
9
0
21
0
0
35
26
B
Rab3c
Serpinb1a
Bves
Pgr
Ankrd34b
Usp31
Ptar1
Slc17a6
Apold1
Nsf
Lpin1
Ina
Sync
Ube2ql1
Fa2h
Apba1
Glra1
Mobp
Crtac1
Kif5c
Gjd2
Marf1
Ndrg4
Aqp6
Calcb
Fbxo41
Syt7
Enpp2
Ppap2a
Cpm
Calca
Acta1
Lgi2
Ppapdc3
Nrsn1
Srebf2
Dusp1
Timm22
Ankrd55
Nmnat2
Vgf
Rhd
Runx1t1
Kif5a
Uchl1
Spag5
Ccdc148
Tenm4
Slc32a1
Csf
Apln
Smyd1
Spock2
Lamp5
Dnm1
Mal2
Sh3bgr
Unc13a
Kcnh2
Ppargc1b
Unc13c
Synj1
Rit2
Hs6st2
Cacna2d2
Spock3
Ank3
Panx2
Reln
Mc4r
S100b
Dlk1
Rims2
Sc5d
Hmgcr
Ptch1
Grm3
Hoxc8
Hmgcs1
Cyp51
Insig1
Lss
Mvd
Fdft1
Nsdhl
Elovl6
Arl1l
Itgb4
Syt4
Acly
Acvr1c

Legends to Supplementary Figures

Figure S1. Biodistribution analysis of miR after intranasal delivery. (**A-C**) The distribution of Cy3-labeled miR was examined throughout the neuroaxis by confocal microscopy. Cy3-miR were detected in all regions of the brain (**A**), the dorsal (DWM) and ventral (VWM) white matter spinal cord (SC) (**B**), and all cell types of the CNS: GFAP+ astrocytes, Iba+ microglia, NeuN+ neurons, and proteolipid PLP+ OLs (**C**). (n = 3 mice). (**D**) Confocal micrographs of Cy3 labeled-miR (arrows) distributed by intranasal delivery in different regions of the CNS. Nuclei stained with DAPI (blue), bar = 20 μm.

Figure S2. miR-219 reduces gliosis, fibrinogen leakage, and TMEV immunoreactivity. Representative confocal micrographs of Iba1+ microglia (**A**), and GFAP+ astrogliosis (**B**) in thoracic spinal cord sections. (**C**) Blood-brain barrier (BBB) permeability assessed by parenchymal fibrinogen staining (arrows) in thoracic spinal cord. (**D**) Representative confocal micrographs of BeAn capsid staining in thoracic spinal cord. Nuclei were stained with TO-PRO3 (red). Experimental groups: control (Ct) and mice with chronic demyelination treated with vehicle (TMEV+veh), scrambled miR (TMEV+miR-scr) or miR-219 (TMEV+miR-219). Nuclei stained with DAPI (blue), bar = 20 μm.

Figure S3. miR-219 potentiates transcriptional changes in cholesterol-related genes. (**A**) A heat-map of differentially expressed transcripts in in thoracic spinal cord of experimental groups. (**B**) GO analysis of the biological processes for gene clusters identified in (**A**). (**C**) Venn diagram showing overlap of genes from Cluster 1 and predicted targets for miR-219 by TargetScan. Experimental groups consist of healthy

mice (control) and mice with chronic demyelination treated with vehicle (TMEV+veh), scrambled miR (TMEV+miR-scr) or miR-219 (TMEV+miR-219).

Figure S4: Venn diagram comparing Cluster 1 with downregulated genes in OPCs and OLs treated with miR-219. (**A**) Genes related to cholesterol biosynthesis (GO analysis) from Cluster 1 in TMEV-infected animals treated with miR-219 compared with genes downregulated in OPCs and OLs treated with miR-219. (**B**) Gene network and enrichment analysis of Cluster 1 identified by STRING[1]. Functional interactions between cholesterol-related genes from Cluster 1 are the main connected component of the gene network analysis. These functional interactions were not present in OPCs and OLs treated with miR-219

References:

1. Szklarczyk, D, Morris, JH, Cook, H, Kuhn, M, Wyder, S, Simonovic, M, *et al*. (2017). The STRING database in 2017: quality-controlled protein–protein association networks, made broadly accessible. *Nucleic Acids Res*. **45**(D1):D362-D368